

Gallic Acid Impedes Non-Small Cell Lung Cancer Progression via Suppression of EGFR-Dependent CARM1-PELP1 Complex

This article was published in the following Dove Press journal:
Drug Design, Development and Therapy

Dong Wang¹
Burenbatu Bao²

¹Department of Oncology of Mongolian-Western Medicine, Affiliated Hospital of Inner Mongolia University for Nationalities, Tongliao 028007, People's Republic of China; ²Department of Mongolian Medicine Hematology & Oncology, Affiliated Hospital of Inner Mongolia University for Nationalities, Tongliao 028007, People's Republic of China

Background: Non-small cell lung cancer (NSCLC) is a common cause of cancer-related deaths. This study identified the regulatory pattern of gallic acid in NSCLC.

Methods: Human NSCLC cells were treated with different doses of gallic acid, after which, MTT assay and flow cytometry were performed to determine the survival and apoptotic rate of human NSCLC cells. Then, co-immunoprecipitation assay was performed to analyze the relationships between gallic acid, epidermal growth factor receptor (EGFR), and CARM1-PELP1. Next, we analyzed whether PELP1, CARM1 and EGFR were associated with the effects of gallic acid on NSCLC cells by conducting rescue experiments. The expression pattern of phosphorylated EGFR, EGFR, Ki67, as well as Fas, FasL and Caspase 3 proteins in cancer cells or xenografts was measured by Western blot analysis. Lastly, the role of gallic acid in the tumor growth was assessed in nude mice.

Results: The ideal dose of gallic acid that presented good suppressive effect on NSCLC cells were 30 μ M, 50 μ M and 75 μ M, respectively. Gallic acid played an inhibiting role in the activation of EGFR, which further reduced the formation of CARM1-PELP1 complex, ultimately repressed the proliferation and elevated apoptosis of NSCLC cells. Meanwhile, CARM1 repression led to decreased growth, proliferation and migration abilities of NSCLC cells. Animal experiments confirmed that gallic acid contributed to the inhibition of tumor growth in vivo.

Conclusion: To sum up, gallic acid could potentially prevent NSCLC progression via inhibition of EGFR activation and impairment of the binding of CARM1 to PELP1, highlighting a novel therapy to dampen NSCLC progression.

Keywords: gallic acid, EGFR, CARM1, PELP1, non-small cell lung cancer, CARM1-PELP1 complex

Introduction

Non-small-cell lung cancer (NSCLC) is the main cause of cancer-related deaths, compromising 85% of the newly diagnosed lung cancer.¹ Among these patients, over 65% exhibited locally advanced or metastatic disease.² Based on the in-depth understanding of lung cancer genomes, NSCLC is a distinct disease with genetic and cellular heterogeneity, which is attributed to genetic mutations, like epidermal growth factor receptor (EGFR), anaplastic lymphoma kinase (ALK), and ROS1 receptor tyrosine kinase.³ Great achievements have been made for NSCLC treatment, such as targeted therapies (targeting EGFR, ALK, and ROS1) and immunotherapy, which can increase the survival of NSCLC patients.⁴ However, acquired resistance may pose a major clinical challenge to the targeted cancer treatment.²

Correspondence: Burenbatu Bao
Department of Mongolian Medicine
Hematology & Oncology, Affiliated
Hospital of Inner Mongolia University for
Nationalities, No. 1742, Huolinhe Street,
Horqin District, Tongliao 028007, Inner
Mongolia, People's Republic of China
Tel/Fax +86-475-8215816
Email wangdong7776@126.com

Gallic acid is a trihydroxybenzoic acid that can be found in several herbal medicine, food, and beverages. Apart from its antitumor potential against cancer, it also plays a functional role in diabetes, hypercholesterolemia, cardiac hypertrophy, fibrosis, and hypertension due to its excellent oxidation resistance.^{5,6} Gallic acid has been demonstrated to inhibit EGFR, which in turn suppresses NSCLC progression in certain condition.⁷ EGFR is implicated in the pathogenesis of several types of cancers such as colorectal cancer and liver cancer.^{8,9} However, the research of EGFR in NSCLC gained the most attention due to its outstanding therapeutic effects. As we mentioned above, more researches have been conducted to overcome its resistance to inhibitors. For example, TWIST1, the epithelial–mesenchymal transition (EMT) transcription factor has been demonstrated to effectively minimize the resistance to EGFR tyrosine kinase inhibitors.¹⁰ EGFR and PELP1 are associated with the ER-activated signaling, whose inhibition represents a novel method to circumvent hormone resistance in breast cancer.¹¹ Meanwhile, CARM1 and PELP1 have been revealed to bind to each other, and inhibition of CARM1 could reduce the carcinogenic function of PELP1 in vitro.¹² In addition, another study suggested that the repression of CARM1 was a potential therapy in NSCLC.¹³ Hence, it is reasonable to refer that the suppression of CARM1-PELP1 complex may play an anti-tumor role in NSCLC. Since the molecular mechanism underlying gallic acid in NSCLC still largely unknown, this study aimed to explore the possible relationship among gallic acid, EGFR and CARM1-PELP1 complex in NSCLC and their impacts on the NSCLC progression to provide a better understanding for the development of novel therapy for NSCLC treatment.

Materials and Methods

Ethics Statement

The current study was performed with the approval of the Animal Ethics Committee of the Affiliated Hospital of Inner Mongolia University for Nationalities. All animal experiments were performed in strict accordance with the recommendations in the Guide for the Care and Use of Laboratory Animals of the National Institutes of Health.

Cell Culture and Transfection

Human normal lung epithelial cell line (BEAS-2B) and human NSCLC cell lines A549 and NCI-H1299 were purchased from National Infrastructure of Cell Line Resource (<http://www.cellresource.cn/index.aspx>) and cultured, respectively, in

Ham's F12K medium (21127022, GIBCO BRL, Grand Island, NY, USA) supplemented with 10% fetal bovine serum (FBS) (GIBCO BRL, Grand Island, NY, USA), 100 µg/mL streptomycin, 100 U/mL penicillin in 95% saturated humidity at 37°C with 5% CO₂.

The cells were transfected with plasmid overexpressing PELP1 (oe-PELP1), short hairpin RNA (shRNA) targeting PELP1 (sh-PELP1) or their corresponding negative controls (NC) as per the instructions of Lipofectamine 2000 (Invitrogen, Carlsbad, CA, USA). The overexpression vectors were designed and constructed by Shanghai GenePharma Co., Ltd. (Shanghai, China) using pcDNA3.1 and pRNAT-U6.1/neo, respectively.

Western Blot Analysis

Total proteins were isolated from tissues and cells using radioimmunoprecipitation assay (RIPA) lysis buffer containing phenylmethylsulfonyl fluoride (PMSF). Then, 50 µg of protein was separated by sodium dodecyl sulfate-polyacrylamide gel electrophoresis and transferred onto the polyvinylidene fluoride membranes. The membranes were incubated overnight at 4°C with the following diluted primary antibodies from Abcam Inc. (Cambridge, UK): rabbit polyclonal antibody to phosphorylated EGFR (ab5644, 1:1000), rabbit monoclonal antibody to EGFR (ab52894, 1:1000), rabbit monoclonal antibody to Ki67 (ab16667, 1:1000), rabbit polyclonal antibody to Fas (ab82419, 1:1000), rabbit polyclonal antibody to Fas Ligand (FasL) (ab15285, 1:1000), rabbit anti-Cleaved-caspase 3 (ab2302, 1:1000), rabbit polyclonal antibody to Caspase 3 (ab13847, 1:1000) and rabbit polyclonal antibody to β-actin (ab227387, 1:500). After three washes with Tris-buffered saline Tween-20 (TBST) (10 min/time), the membranes were incubated with horseradish peroxidase-labeled secondary antibody goat anti-rabbit immunoglobulin G (IgG, ab97051, 1:2000, Abcam Inc., Cambridge, UK). The immunocomplexes on the membrane were visualized using enhanced chemiluminescence reagent (BB-3501, Amersham Pharmacia Biotech, Amersham, UK) and band intensities were quantified using Bio-Rad imaging system (Bio-Rad Laboratories, Hercules, CA, USA) and Quantity One v4.6.2 software. The ratio of the gray value of the target band to β-actin was representative of the relative protein expression.

Coimmunoprecipitation (Co-IP) Assay

The cells were lysed at 4°C for 30 mins in RIPA buffer (Thermo Fisher Scientific, Waltham, MA, USA) and

centrifuged at 1300 g for 30 mins at 4°C. Subsequently, the specific antibody was mixed with the supernatant at 4°C overnight, followed by the addition of Pierce protein A/G Magnetic Beads (88803, Thermo Fisher Scientific, Waltham, MA, USA) for 4 h of incubation at 4°C. Finally, the beads following centrifugation were washed and mixed with the loading buffer, then subjected to SDS-PAGE and immunoblotting (IB) analysis.

MTT Assay

A549 and NCI-H1299 cells were inoculated into a 96-well plate. After the cells adhered to the wall, gallic acid with different concentration was added. After the culture solution was discarded, 200 µL of serum-free culture medium containing 20 µL of MTT was added to the cells and incubated at 37°C for 4 h. Lastly, 150 µL of dimethyl sulfoxide (DMSO) was added to the cells and incubated for 10 min. The absorbance value was then measured at a wavelength of 495 nm.

Flow Cytometry

A549 and NCI-H1299 cells were seeded into a 6-well plate at a cell density of 5×10^5 cells/mL, with 2 mL of single-cell suspension per well. After the cells adhered to the wall, the medium was aspirated and discarded. The cells were treated with gallic acid diluted in serum-free medium for 24 h. The cells in the control group were added with an equal volume of serum-free culture solution. The cells were then collected, trypsinized, followed by the addition of 100 µL binding buffer. Next, 10 µL of Annexin V-FITC staining solution and 10 µL of propidium iodide (PI) staining solution (Beyotime, Shanghai, China) were added to the cells and incubated for 10 min. Subsequently, the cells were centrifuged at a low speed and the supernatant was discarded. The cells were then mixed completely with 400 µL of binding buffer and the apoptotic rate was detected by flow cytometry.

Cell Migration Test

Cell migration was measured according to a QCM Colorimetric Cell Migration Assay Kit. Briefly, the cells following 48 h of transfection were collected and made into cell suspension, which was subsequently loaded onto the apical chamber. Next, 50 µL of culture solution containing 10% FBS was added to the basolateral chamber. After 18 h of treatment with DMSO or CARM1 inhibitor, AMI-1 (10 µM, ALX-270-440, Enzo Biochem Inc., New York, NY, USA), the migrated cells were stained and the absorbance was measured at 595 nm.

Nude Mouse Xenograft Model of NSCLC

A total of 40 BALB/C nude mice (4 weeks old, weighing 18–22 g) were purchased from the Experimental Animal Center of Inner Mongolia Medical University. Under sterile conditions, 0.2 mL of cell suspension (1×10^7 cells/mL) was pipetted with a 1 mL disposable syringe and slowly injected into the right armpit of the nude mouse. The long diameter of the tumor block >5 mm and felted lumps was indicative of the successful establishment of the NSCLC mouse model. After successful modeling, 0 µg/kg, 10 µg/kg, 20 µg/kg and 40 µg/kg of gallic acid were injected subcutaneously into the back of the neck of nude mice for 14 d (1 time/d). After administration, each mouse was intraperitoneally injected with 0.5% heparin (0.5 mL) for heparinization and then ocular blood samples were collected. The concentration of alanine aminotransferase (ALT), gamma-glutamyltransferase (γ-GT), blood urea nitrogen (BUN) and creatinine (Cr) were then detected after centrifugation. During the administration, the long diameter and short diameter of the transplanted tumors were measured by vernier calipers every 2 d, which was repeated in triplicate to obtain the average values. The tumor volume was then calculated: $V = \text{long diameter} \times \text{short diameter}^2/2$ and the growth curve of the transplanted tumors were plotted based on the values obtained. After 14 d, the nude mice were weighed and euthanized with carbon dioxide asphyxiation and the tumor was removed and weighted.

Statistical Analysis

SPSS 21.0 statistical software (IBM Corporation, Armonk, NY, USA) was used for the statistical analyses. The measurement data were expressed as mean ± standard deviation. Data obeying normal distribution and homogeneity of variance between two groups were analyzed by unpaired *t*-test and data among multiple groups were compared using one-way analysis of variance (ANOVA), followed by a Tukey's multiple comparisons post hoc test. Data at different time points were compared by repeated-measures ANOVA, followed by Bonferroni's post hoc test. A value of $p < 0.05$ was considered statistically significant.

Results

Gallic Acid Disrupts the Activation of EGFR and Suppresses NSCLC Cell Viability

To investigate the effect of gallic acid on apoptosis of NSCLC cells, the A549 and NCI-H1299 cells were treated with low-dose, medium-dose and high-dose of gallic acid. According to the preliminary experiment results, the doses

(0 μ M, 30 μ M, 50 μ M and 75 μ M) which presenting better inhibitory effects on A549 and NCI-H1299 cells were selected for further experimental use.

The viability of A549 and NCI-H1299 cells was detected by MTT assay. The results showed that compared with control cells, the viability of A549 and NCI-H1299 cells treated with different doses of gallic acid (30 μ M, 50 μ M and 75 μ M) was lower at 12 h, 24 h and 48 h post transfection, respectively ($p < 0.05$) (Figure 1A). The apoptotic rate of A549 and NCI-H1299 cells were subsequently detected by flow cytometry. Compared with the apoptotic rate of cells treated with 0 μ M gallic acid (5.27%/4.53%), higher apoptotic rates were observed in the cells treated with gallic acid at low-dose (30 μ M), medium-dose (50 μ M) and high-dose (75 μ M) which were 11.65%/9.37%, 16.83%/13.15% and 21.98%/18.86%, correspondingly ($p < 0.05$) (Figure 1B), showing increases in a dose-dependent manner. To investigate the possible effect of gallic acid on EGFR, further EGFR phosphorylation and protein expression of EGFR, Ki67, Fas, FasL and Cleaved-caspase 3 in A549 and NCI-H1299 cells treated with 30 μ M, 50 μ M and 75 μ M gallic acid were detected by Western blot analysis. Results revealed that compared with the cells treated by 0 μ M gallic acid, the extent of EGFR phosphorylation and protein expression of Ki67 in the cells treated with low-, medium- and high-dose of gallic acid were decreased, while the protein expression of Fas, FasL and Cleaved-caspase 3 was increased (both $p < 0.05$) (Figure 1C). The above results indicated that gallic acid

poses an inhibitory effect on NSCLC cell growth which might be achieved by blocking the activation of EGFR.

Activation of EGFR Promotes the Formation of CARM1-PELP1 Complex

Based on previous literature,^{12,14} we hypothesized that gallic acid may inhibit the formation of CARM1-PELP1 complex by suppressing EGFR signaling pathway, thus decelerating the carcinogenic function of PELP1.

To testify the proposed hypothesis, the binding of CARM1 to PELP1 in A549 cells was assessed by Co-IP assay. The results showed that CARM1 and PELP1 bound to each other in A549 cells (Figure 2A). Next, in order to verify the effect of EGFR signaling pathway on the binding of CARM1 and PELP1, A549 cells were serum-starved for 24 h and treated with EGF (100 ng/mL) for 8 h. Western blot analysis showed the extent of EGFR phosphorylation in the cells treated with EGF was higher than that in cells treated by DMSO ($p < 0.05$) (Figure 2B). Results from Co-IP assay indicated that the binding of CARM1 to PELP1 was enhanced in A549 cells treated with EGF as compared to cells treated with DMSO (Figure 2C).

CARM1-PELP1 Complex Promotes the Carcinogenic Activity of PELP1

In order to detect whether CARM1 was essential for the carcinogenic properties of PELP1, A549 and NCI-H1299 cells were transfected with oe-PELP1 or sh-PELP1 every 2 d, followed by treatment with CARM1 inhibitor AMI-1

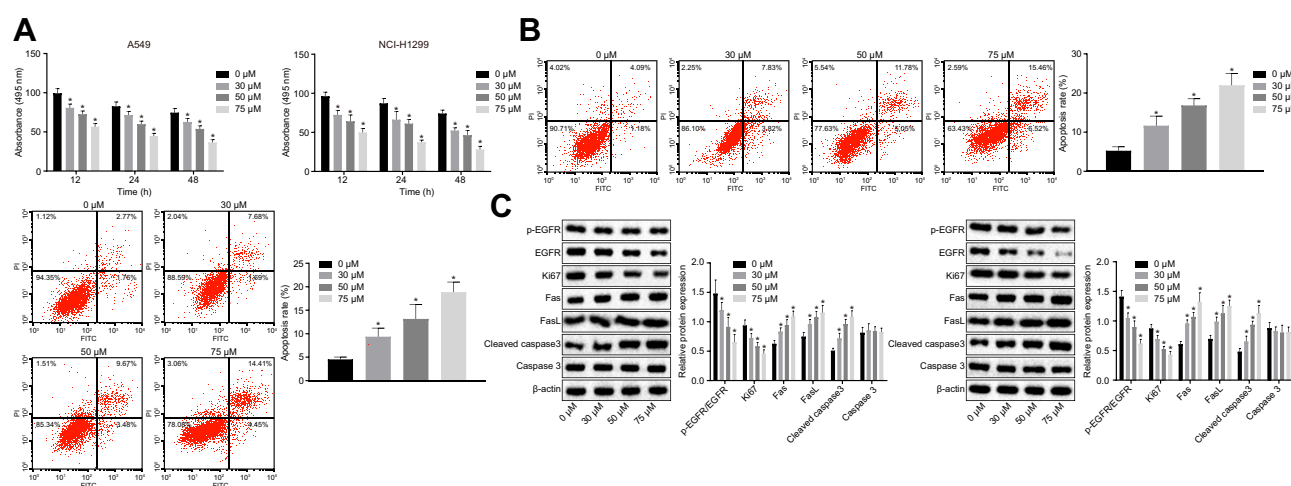


Figure 1 Gallic acid inhibited the development of NSCLC and repressed EGFR activation. (A) The viability of A549 and NCI-H1299 cells detected by MTT assay. (B) The apoptotic rate of A549 and NCI-H1299 cells detected by flow cytometry. (C) Western blot analysis of phosphorylated EGFR, EGFR, Ki67, Fas, FasL and Cleaved-caspase 3 proteins in A549 and NCI-H1299 cells. * $p < 0.05$ vs. the control cells (0 μ M of gallic acid). The above results were all measurement data and expressed as mean \pm standard deviation. Comparisons among multiple groups were analyzed using one-way ANOVA, followed by a Tukey's multiple comparisons post hoc test. The cell experiment was independently repeated three times.

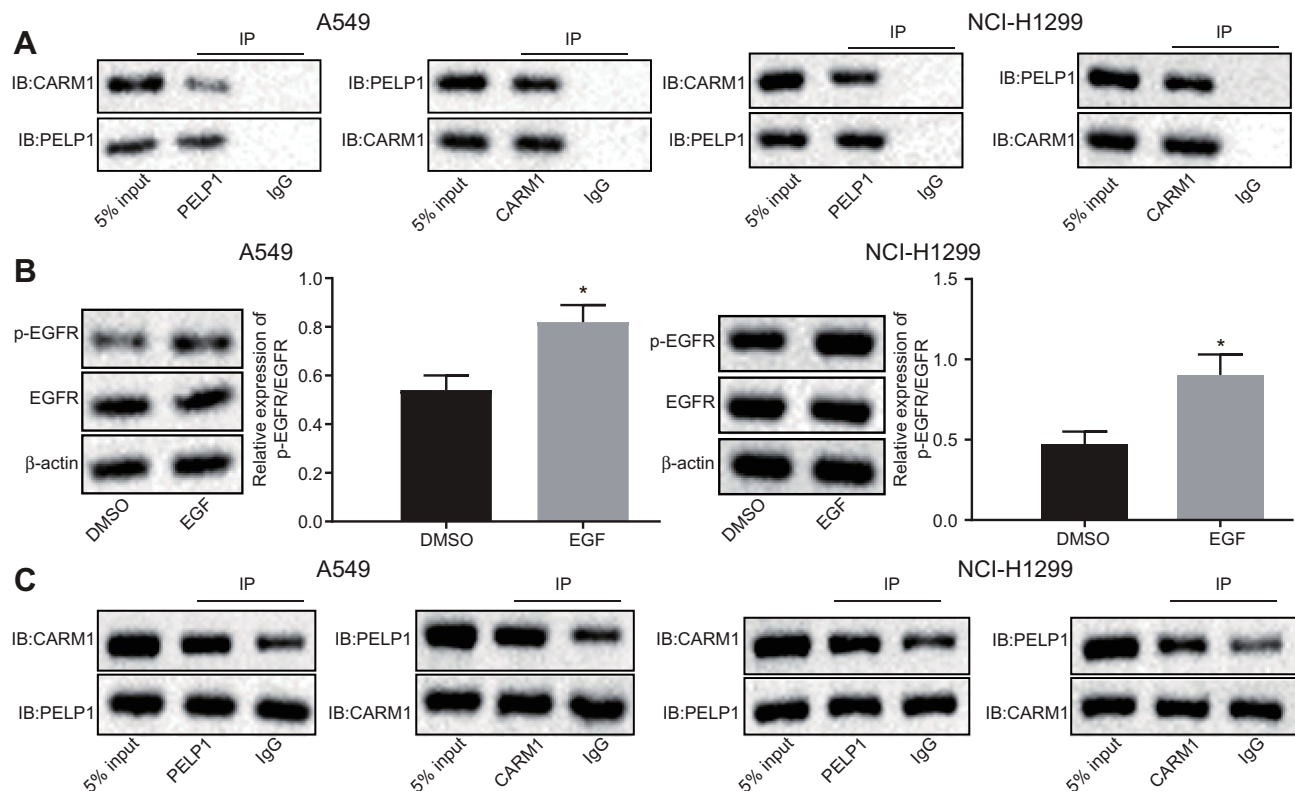


Figure 2 The binding of CARM1 and PELP1 was enhanced by EGFR activation. **(A)** The binding of CARM1 to PELP1 detected by Co-IP assay. **(B)** Western blot analysis of EGFR protein in EGF-treated A549 cells. **(C)** The binding of CARM1 to PELP1 in EGF-treated A549 cells detected by Co-IP assay. * $p < 0.05$ vs. cells treated with DMSO. The above results were all measurement data and expressed as mean \pm standard deviation. Comparisons between two groups were analyzed using the unpaired t-test. Comparisons among multiple groups were analyzed using one-way ANOVA, followed by a Tukey's multiple comparisons post hoc test. The cell experiment was independently repeated three times.

(0 μ M, 1 μ M, 10 μ M and 20 μ M). After 7 d, the viability of A549 and NCI-H1299 cells was detected by MTT assay. The results showed that PELP1 overexpression enhanced the

growth of A549 and NCI-H1299 cells, whereas, inhibition of CARM1 resulted in reduced PELP1-mediated viability of A549 and NCI-H1299 cells (Figure 3A). Then, A549 and

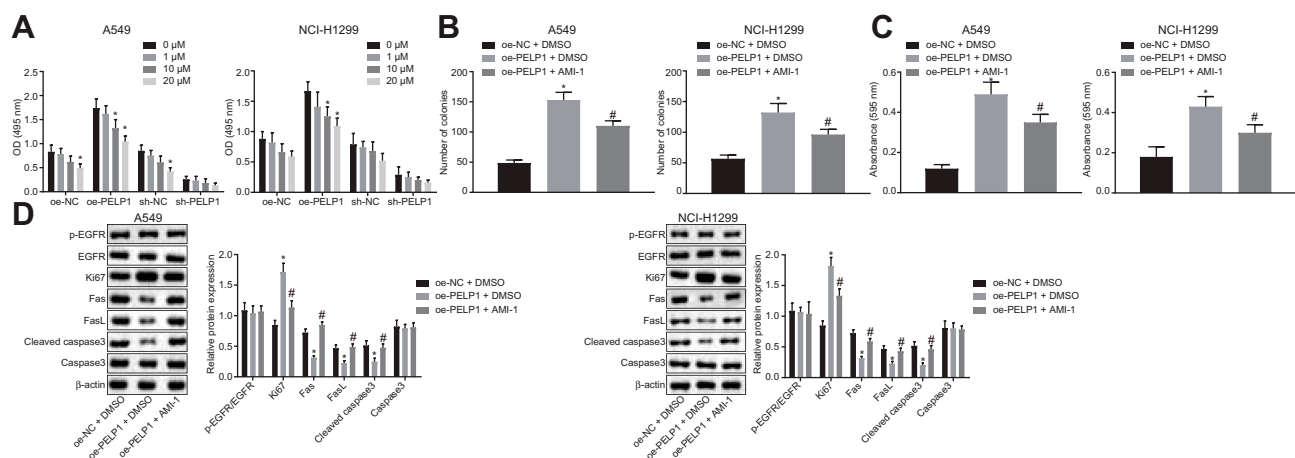


Figure 3 CARM1 positively regulates the carcinogenic activity of PELP1. **(A)** Cell viability of A549 and NCI-H1299 cells detected by MTT assay. * $p < 0.05$ vs. the control cells (0 μ M of gallic acid). **(B)** Colony formation abilities of A549 and NCI-H1299 cells assessed by clonogenic assay. * $p < 0.05$ vs. cells treated by oe-NC plasmid and DMSO, # $p < 0.05$ vs. cells treated by oe-PELP1 plasmid and DMSO. **(C)** Migration ability of A549 and NCI-H1299 cells assessed by QCM Colorimetric Cell Migration Assay. * $p < 0.05$ vs. cells treated by oe-NC plasmid and DMSO, # $p < 0.05$ vs. cells treated by oe-PELP1 plasmid and DMSO. **(D)** Western blot analysis of phosphorylated EGFR, EGFR, Ki67, Fas, FasL and Cleaved-caspase 3 proteins in A549 and NCI-H1299 cells. * $p < 0.05$ vs. cells treated by oe-NC plasmid and DMSO, # $p < 0.05$ vs. cells treated by oe-PELP1 plasmid and DMSO. The above results were all measurement data and expressed as mean \pm standard deviation. Comparisons among multiple groups were analyzed using one-way ANOVA, followed by a Tukey's multiple comparisons post hoc test. The cell experiment was independently repeated three times.

NCI-H1299 cells were transfected with oe-PELP1 every 2 d, and then added with AMI-1 with a final concentration of 10 μ M and treated for 12 d, followed by determination of the colony formation of A549 and NCI-H1299 cells using clonogenic assay. Results suggested that PELP1 overexpression enhanced the proliferation of A549 and NCI-H1299 cells, while inhibition of CARM1 resulted in reduced PELP1-mediated colony formation of A549 and NCI-H1299 cells (Figure 3B).

Subsequently, the A549 and NCI-H1299 cells were transfected with oe-PELP1 and simultaneously treated with either DMSO or AMI-1. The migration ability was measured using QCM Colorimetric Cell Migration Assay Kit. Results showed that PELP1 overexpression elevated the migration of A549 and NCI-H1299 cells, but inhibition of CARM1 suppresses PELP1-mediated migration of A549 and NCI-H1299 cells (Figure 3C). Then, Western blot analysis showed that the expression of Ki67 was increased, while that of Fas, FasL and Cleaved-caspase 3 proteins was decreased by PELP1 overexpression in A549 and NCI-H1299 cells ($p < 0.05$). On the contrary, the changes in the expression of Ki67, Fas and FasL proteins were all reversed by inhibition of CARM1 ($p < 0.05$) (Figure 3D). To sum up, the increase of CARM1-PELP1 complex could enhance the carcinogenesis of PELP1.

Gallic Acid Impedes the Formation of CARM1-PELP1 Complex in a Dose-Dependent Manner

To investigate the effect of gallic acid treatment on the binding of CARM1 to PELP1, the A549 and NCI-H1299 cells were treated by low-dose (30 μ M), medium-dose (50 μ M), and high-dose (75 μ M) of gallic acid, respectively. Results from immunoprecipitation experiments revealed that the CARM1 proteins immunoprecipitated by PELP1 were decreased as the dose of gallic acid increased (Figure 4). Therefore, it was suggested that gallic acid could negatively mediate the formation of CARM1-PELP1 complex.

Gallic Acid Inhibits the Growth of NSCLC Xenografts in vivo

In order to explore the effect of gallic acid on NSCLC in vivo, the nude mice were treated with 10 μ g/kg, 20 μ g/kg, and 40 μ g/kg of gallic acid, respectively. As shown in Figure 5A–C, the average volume and weight of tumors in nude mice were reduced by treatment with 10 μ g/kg, 20 μ g/kg, and 40 μ g/kg gallic acid ($p < 0.05$). The body weight of nude mice showed no significant difference between the control mice and the mice treated with different doses of gallic acid ($p > 0.05$). Then, the extent of EGFR phosphorylation, and expression of EGFR, Ki67, Fas, FasL

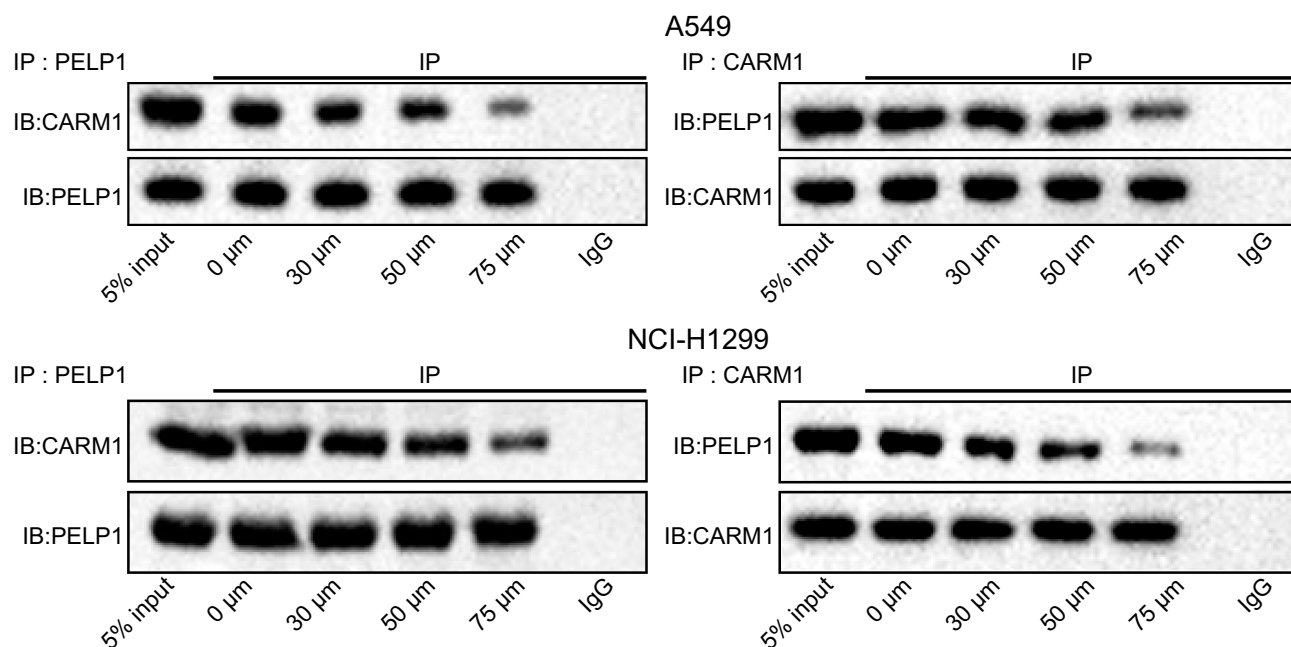


Figure 4 Higher dosage of Gallic acid resulted in weaker binding of CARM1 to PELP1. The binding of CARM1 to PELP1 was detected in the A549 and NCI-H1299 cells treated with Gallic acid at different dosages by Co-IP experiment.

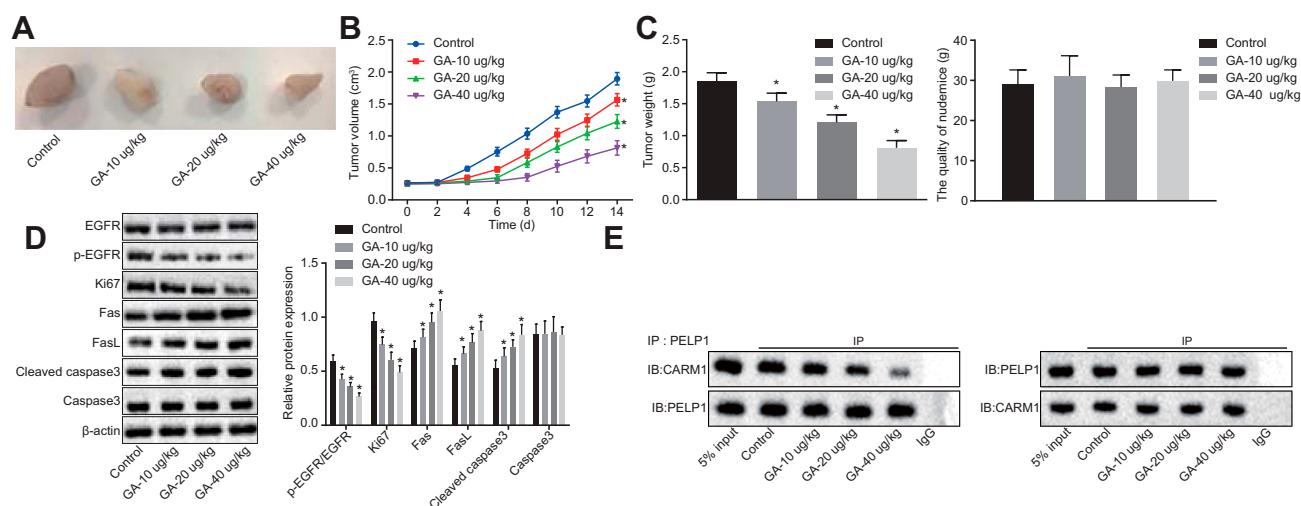


Figure 5 The growth of NSCLC xenografts was suppressed by gallic acid. **(A and C)** Representative images of xenograft tumors and quantitative analysis of body weight and tumor weight after treatment of 10 $\mu\text{g/kg}$, 20 $\mu\text{g/kg}$, and 40 $\mu\text{g/kg}$ of gallic acid. **(B)** Volume data of the transplanted tumors at different time points after treatment with 10 $\mu\text{g/kg}$, 20 $\mu\text{g/kg}$, and 40 $\mu\text{g/kg}$ of gallic acid. **(D)** Western blot analysis of phosphorylated EGFR, EGFR, Ki67, Fas, FasL and Cleaved caspase 3 proteins in transplanted tumors. **(E)** The binding of CARM1 to PELP1 in nude mice treated with 10 $\mu\text{g/kg}$, 20 $\mu\text{g/kg}$, and 40 $\mu\text{g/kg}$ of gallic acid detected by Co-IP assay. The above results were all measurement data and expressed as mean \pm standard deviation. Data comparison in panel B was performed by repeated measurement ANOVA, followed by Bonferroni's post hoc test. Data in panel C and D were analyzed using one-way ANOVA, followed by Tukey's multiple comparisons post hoc test. * $p < 0.05$ vs. the control mice (without treatment of gallic acid). Comparisons between two groups were analyzed using an unpaired t-test, comparisons among multiple groups were analyzed using one-way ANOVA, followed by a Tukey's multiple comparisons post hoc test. Comparisons at different time points were performed by repeated-measures ANOVA, followed by Bonferroni's post hoc test, $n = 10$.

and Cleaved caspase-3 proteins in transplanted tumor tissues from the mice treated with 10 $\mu\text{g/kg}$, 20 $\mu\text{g/kg}$, and 40 $\mu\text{g/kg}$ of gallic acid was detected by Western blot analysis. The results indicated that the EGFR phosphorylation level and protein expression of Ki67 in the mouse tumor tissue xenografts were decreased while the expression of Fas, FasL and Cleaved-caspase 3 proteins was elevated by treatment with 10 $\mu\text{g/kg}$, 20 $\mu\text{g/kg}$ and 40 $\mu\text{g/kg}$ gallic acid, respectively (all $p < 0.05$) (Figure 5D). We further observed the effects of gallic acid treatment on the liver and kidney functions of nude mice (Table 1). Finally, the binding of CARM1 to PELP1 in the nude mice treated with 10 $\mu\text{g/kg}$, 20 $\mu\text{g/kg}$, and 40 $\mu\text{g/kg}$ of gallic acid was weakened in a dose-dependent manner (Figure 5E). Taken together, gallic acid plays an inhibitory role in the tumor growth of NSCLC.

Discussion

NSCLC is the most common malignancy accounting for over 80% of all lung cancers worldwide, which is paralleled with the mutations of various oncogenic drivers such as EGFR and KRAS.¹⁵ Interestingly, gallic acid, a common phenolic compound found in gallnuts, oak bark, sumac, grapes and tea leaves, has been identified to be a potent antioxidant drug and also been revealed to possess superb anti-tumor property.¹⁶ However, the study of gallic acid on NSCLC is insufficient and the molecular mechanism

underlying the roles gallic acid played in NSCLC remains largely unknown. Hence, this study was designed to investigate the mechanism of gallic acid involved in NSCLC. Collectively, the data obtained suggested that gallic acid could potentially inhibit the activity of EGFR and further reduce the formation of CARM1-PELP1 complex, which ultimately impeding the NSCLC progression.

Initial results presented that after gallic acid treatment, the viability of NSCLC cells was decreased and the apoptotic rate was increased, while the activity of EGFR was decreased. A similar finding has also been concluded in other cancer cells, for instance, gallic acid has been confirmed to restrain the activation of EGFR and promote the apoptosis of mesothelioma cells and breast cancer cells.^{17,18} EGFR, a member of ERBB family whose mutations have been illustrated to be associated with the pathogenesis of several kinds of cancers, such as lung cancer and breast cancer, is responsible for 20% of NSCLC.^{19,20} Besides, EGFR has been confirmed to be inhibited by gallic acid, which acts to suppress the progression of breast cancer.¹⁸ We found that phosphorylation of EGFR and expression of Ki67 protein were reduced but the expression of Fas and FasL was augmented in response to gallic acid treatment in this study. Ki67 has been known to be a proliferation marker in the prognosis of cancers.^{21,22} Fas and FasL are two receptors capable of stimulating cell apoptosis.^{23,24} Fas and FasL

Table 1 Liver and Kidney Function of Nude Mice After Treatment with Different Concentration of CA

Group	n	ALT (U/L)	GGT (U/L)	BUN (mmol/L)	Cr (μ mol/L)
Control	10	55.85 \pm 6.39	59.15 \pm 5.29	6.26 \pm 0.52	56.68 \pm 4.73
CA-10 μ g/kg	10	54.06 \pm 4.51	57.82 \pm 6.74	6.18 \pm 0.71	55.12 \pm 3.55
CA-20 μ g/kg	10	52.17 \pm 5.53	55.16 \pm 8.15	6.12 \pm 0.94	54.36 \pm 4.12
CA-40 μ g/kg	10	51.03 \pm 3.98	53.74 \pm 6.07	6.09 \pm 0.76	52.25 \pm 6.38

Abbreviations: ALT, alanine aminotransferase; γ -GT, gamma-glutamyltransferase; BUN, blood urea nitrogen; Cr, creatinine.

have been illustrated previously to be increased by gallic acid, thereby inducing apoptosis of lung fibroblasts.²⁵ Therefore, the above-mentioned results suggested the suppressive effect of gallic acid on the progression of NSCLC through inhibition of EGFR.

We also found that the activation of EGFR resulted in increased formation of CARM1-PELP1 complex, which could further promote the oncogenicity of PELP1. In addition, the inhibition of CARM1 has led to decreased proliferative, colony formation and migration capacities of NSCLC cells transfected with PELP1 overexpression, thus reversing the oncogenic role of PELP1. Additionally, AMI-1 (inhibitor of CARM1) has been observed to reverse the effect of PELP1.²⁶ CARM1, also known as coactivator-associated arginine methyltransferase 1, has been reported to act as a tumor stimulator in many cancers. For example, the up-regulation of CARM1 has been demonstrated to promote the development of breast cancer and worsen the prognosis, causing shorter survival of breast cancer patients.^{27,28} Besides, another study has also suggested its oncogenic role in NSCLC progression.¹³ PELP1, as a crucial coactivator of the ER signaling pathway, has been observed to highly express in NSCLC cells, where ER signaling pathway involved in the promotion of lung

cancer progression.²⁹ More importantly, both CARM1 and PELP1 have been identified to bind to each other, while the inhibition of CARM1 could weaken the carcinogenesis of PELP1 dramatically.¹² The aforementioned results indicated that the inhibition of CARM1-PELP1 complex formation may contribute to the suppression of NSCLC progression.

Another important finding was that gallic acid diminished the formation of CARM1-PELP1 complex in a dose-dependent manner. The results from Co-IP assay presented that an increased dose of gallic acid resulted in reduced CARM1-PELP1 complex formation. Therefore, it can be referred that gallic acid might inhibit the formation of CARM1-PELP1 complex to prevent cancer progression, which might be achieved by inhibiting the activation of EGFR. Gallic acid dose-dependent property has been demonstrated to decrease the growth of lung cancer cell.³⁰ Furthermore, the anti-cancer property of gallic acid has also been reported in A549, a human lung adenocarcinoma cell line, in a dose-dependent manner.³¹ Importantly, gallic acid has the capacity to inhibit the tumor growth of NSCLC cells in xenograft models in vivo.³² Therefore, the aforementioned results were in consistent with our findings that gallic acid could potentially inhibit the tumor growth of NSCLC.

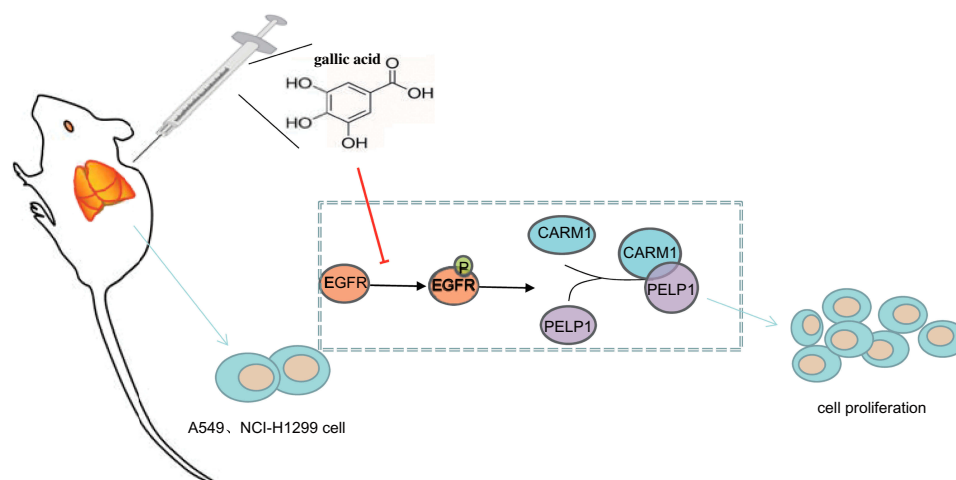


Figure 6 A mechanism map depicting the role of gallic acid in the progression of NSCLC via EGFR-CARM1-PELP1 axis. Gallic acid disrupts the activation of EGFR to inhibit the binding of CARM1 to PELP1, whereby inhibiting the carcinogenic activity of PELP1 and repressing the development of NSCLC.

Conclusion

In summary, this study has shown that gallic acid could inhibit the carcinogenic activity of PELP1 and suppress the development of NSCLC by inhibiting the activation of EGFR and the formation of CARM1-PELP1 complex (Figure 6). Hence, it is speculated that gallic acid might be a novel therapeutic candidate for treating NSCLC via impairing EGFR-dependent CARM1-PELP1 formation.

Acknowledgments

We acknowledge and appreciate our colleagues for their valuable efforts and comments on this paper. This work was supported by the Research Program of Science and Technology at Universities of Inner Mongolia Autonomous Region (No: NJZZ20107).

Disclosure

The authors report no conflicts of interest in this work.

References

- Reck M, Rabe KF, Longo DL. Precision diagnosis and treatment for advanced non-small-cell lung cancer. *N Engl J Med*. 2017;377(9):849–861. doi:10.1056/NEJMr1703413
- Reck M, Heigener DF, Mok T, Soria JC, Rabe KF. Management of non-small-cell lung cancer: recent developments. *Lancet*. 2013;382(9893):709–719. doi:10.1016/S0140-6736(13)61502-0
- Chen Z, Fillmore CM, Hammerman PS, Kim CF, Wong KK. Non-small-cell lung cancers: a heterogeneous set of diseases. *Nat Rev Cancer*. 2014;14(8):535–546. doi:10.1038/nrc3775
- Herbst RS, Morgensztern D, Boshoff C. The biology and management of non-small cell lung cancer. *Nature*. 2018;553(7689):446–454. doi:10.1038/nature25183
- Variya BC, Bakrania AK, Madan P, Patel SS. Acute and 28-days repeated dose sub-acute toxicity study of gallic acid in albino mice. *Regul Toxicol Pharmacol*. 2019;101:71–78. doi:10.1016/j.yrtph.2018.11.010
- Jin L, Piao ZH, Sun S, et al. Gallic acid attenuates pulmonary fibrosis in a mouse model of transverse aortic contraction-induced heart failure. *Vascul Pharmacol*. 2017;99:74–82. doi:10.1016/j.vph.2017.10.007
- Nam B, Rho JK, Shin DM, Son J. Gallic acid induces apoptosis in EGFR-mutant non-small cell lung cancers by accelerating EGFR turnover. *Bioorg Med Chem Lett*. 2016;26(19):4571–4575. doi:10.1016/j.bmcl.2016.08.083
- Bertotti A, Papp E, Jones S, et al. The genomic landscape of response to EGFR blockade in colorectal cancer. *Nature*. 2015;526(7572):263–267. doi:10.1038/nature14969
- Ye QH, Zhu WW, Zhang JB, et al. GOLM1 modulates EGFR/RTK cell-surface recycling to drive hepatocellular carcinoma metastasis. *Cancer Cell*. 2016;30(3):444–458. doi:10.1016/j.ccell.2016.07.017
- Yochum ZA, Cades J, Wang H, et al. Targeting the EMT transcription factor TWIST1 overcomes resistance to EGFR inhibitors in EGFR-mutant non-small-cell lung cancer. *Oncogene*. 2019;38(5):656–670. doi:10.1038/s41388-018-0482-y
- Renoir JM, Marsaud V, Lazennec G. Estrogen receptor signaling as a target for novel breast cancer therapeutics. *Biochem Pharmacol*. 2013;85(4):449–465. doi:10.1016/j.bcp.2012.10.018
- Mann M, Cortez V, Vadlamudi R. PELP1 oncogenic functions involve CARM1 regulation. *Carcinogenesis*. 2013;34(7):1468–1475. doi:10.1093/carcin/bgt091
- Wang D, Hu Y. Long non-coding RNA PVT1 competitively binds MicroRNA-424-5p to regulate CARM1 in radiosensitivity of non-small-cell lung cancer. *Mol Ther Nucleic Acids*. 2019;16:130–140. doi:10.1016/j.omtn.2018.12.006
- Manavathi B, Nair SS, Wang RA, Kumar R, Vadlamudi RK. Proline-, glutamic acid-, and leucine-rich protein-1 is essential in growth factor regulation of signal transducers and activators of transcription 3 activation. *Cancer Res*. 2005;65(13):5571–5577. doi:10.1158/0008-5472.CAN-04-4664
- Wood K, Hensing T, Malik R, Salgia R. Prognostic and predictive value in KRAS in non-small-cell lung cancer: a review. *JAMA Oncol*. 2016;2(6):805–812. doi:10.1001/jamaoncol.2016.0405
- Choubey S, Goyal S, Varughese LR, Kumar V, Sharma AK, Beniwal V. Probing gallic acid for its broad spectrum applications. *Mini Rev Med Chem*. 2018;18(15):1283–1293. doi:10.2174/1389557518666180330114010
- Demiroglu-Zergeroglu A, Candemir G, Turhanlar E, Sagir F, Ayvali N. EGFR-dependent signalling reduced and p38 dependent apoptosis required by gallic acid in malignant mesothelioma cells. *Biomed Pharmacother*. 2016;84:2000–2007. doi:10.1016/j.biopha.2016.11.005
- Chen YJ, Lin KN, Jhang LM, Huang CH, Lee YC, Chang LS. Gallic acid abolishes the EGFR/Src/Akt/Erk-mediated expression of matrix metalloproteinase-9 in MCF-7 breast cancer cells. *Chem Biol Interact*. 2016;252:131–140. doi:10.1016/j.cbi.2016.04.025
- Arteaga CL, Engelman JA. ERBB receptors: from oncogene discovery to basic science to mechanism-based cancer therapeutics. *Cancer Cell*. 2014;25(3):282–303. doi:10.1016/j.ccr.2014.02.025
- Roskoski R Jr. Small molecule inhibitors targeting the EGFR/ErbB family of protein-tyrosine kinases in human cancers. *Pharmacol Res*. 2019;139:395–411. doi:10.1016/j.phrs.2018.11.014
- Cuylens S, Blaukopf C, Politi AZ, et al. Ki-67 acts as a biological surfactant to disperse mitotic chromosomes. *Nature*. 2016;535(7611):308–312. doi:10.1038/nature18610
- Leung SCY, Nielsen TO, Zabaglo LA, et al. Analytical validation of a standardised scoring protocol for Ki67 immunohistochemistry on breast cancer excision whole sections: an international multicentre collaboration. *Histopathology*. 2019;75(2):225–235. doi:10.1111/his.13880
- Fu Q, Fu TM, Cruz AC, et al. Structural basis and functional role of intramembrane trimerization of the Fas/CD95 death receptor. *Mol Cell*. 2016;61(4):602–613. doi:10.1016/j.molcel.2016.01.009
- Wang M, Su P. The role of the Fas/FasL signaling pathway in environmental toxicant-induced testicular cell apoptosis: an update. *Syst Biol Reprod Med*. 2018;64(2):93–102. doi:10.1080/19396368.2017.1422046
- Chuang CY, Liu HC, Wu LC, Chen CY, Chang JT, Hsu SL. Gallic acid induces apoptosis of lung fibroblasts via a reactive oxygen species-dependent ataxia telangiectasia mutated-p53 activation pathway. *J Agric Food Chem*. 2010;58(5):2943–2951. doi:10.1021/jf9043265
- Lim CS, Alkon DL. Inhibition of coactivator-associated arginine methyltransferase 1 modulates dendritic arborization and spine maturation of cultured hippocampal neurons. *J Biol Chem*. 2017;292(15):6402–6413. doi:10.1074/jbc.M117.775619
- Habashy HO, Rakha EA, Ellis IO, Powe DG. The oestrogen receptor coactivator CARM1 has an oncogenic effect and is associated with poor prognosis in breast cancer. *Breast Cancer Res Treat*. 2013;140(2):307–316. doi:10.1007/s10549-013-2614-y
- Wang L, Zhao Z, Meyer MB, et al. CARM1 methylates chromatin remodeling factor BAF155 to enhance tumor progression and metastasis. *Cancer Cell*. 2014;25(1):21–36. doi:10.1016/j.ccr.2013.12.007
- Slowikowski BK, Galecki B, Dyszkiewicz W, Jagodzinski PP. Increased expression of proline-, glutamic acid- and leucine-rich protein PELP1 in non-small cell lung cancer. *Biomed Pharmacother*. 2015;73:97–101. doi:10.1016/j.biopha.2015.05.015

30. You BR, Park WH. Gallic acid-induced lung cancer cell death is related to glutathione depletion as well as reactive oxygen species increase. *Toxicol in Vitro*. 2010;24(5):1356–1362. doi:10.1016/j.tiv.2010.04.009
31. Maurya DK, Nandakumar N, Devasagayam TP. Anticancer property of gallic acid in A549, a human lung adenocarcinoma cell line, and possible mechanisms. *J Clin Biochem Nutr*. 2011;48(1):85–90. doi:10.3164/jcbn.11-004FR
32. Ji BC, Hsu WH, Yang JS, et al. Gallic acid induces apoptosis via caspase-3 and mitochondrion-dependent pathways in vitro and suppresses lung xenograft tumor growth in vivo. *J Agric Food Chem*. 2009;57(16):7596–7604. doi:10.1021/jf901308p

Drug Design, Development and Therapy

Dovepress

Publish your work in this journal

Drug Design, Development and Therapy is an international, peer-reviewed open-access journal that spans the spectrum of drug design and development through to clinical applications. Clinical outcomes, patient safety, and programs for the development and effective, safe, and sustained use of medicines are a feature of the journal, which has also

been accepted for indexing on PubMed Central. The manuscript management system is completely online and includes a very quick and fair peer-review system, which is all easy to use. Visit <http://www.dovepress.com/testimonials.php> to read real quotes from published authors.

Submit your manuscript here: <https://www.dovepress.com/drug-design-development-and-therapy-journal>